Received: 24 February 2021 | Accepted: 24 October 2022

DOI: 10.1111/syen.12578

ORIGINAL ARTICLE

Systematic Entomology

Royal Entomological Society

Defensive spines are associated with large geographic range but not diversification in spiny ants (Hymenoptera: Formicidae: *Polyrhachis*)

Benjamin D. Blanchard[1] | **Corrie S. Moreau**[2,3]

[1]CAS Key Laboratory of Tropical Forest Ecology, Xishuangbanna Tropical Botanical Garden, Chinese Academy of Sciences, Menglun, Yunnan, China

[2]Department of Entomology, Cornell University, Ithaca, New York, USA

[3]Department of Ecology and Evolutionary Biology, Cornell University, Ithaca, New York, USA

Correspondence
Benjamin D. Blanchard, CAS Key Laboratory of Tropical Forest Ecology, Xishuangbanna Tropical Botanical Garden, Chinese Academy of Sciences, Menglun, Mengla, Yunnan 666303, China.
Email: bdblanchard@outlook.com

Funding information
Chinese Academy of Sciences, Grant/Award Number: 2021PB0085; Division of Environmental Biology, Grant/Award Numbers: DEB-1701352, DEB-1900357; Division of Integrative Organismal Systems, Grant/Award Number: IOS-1916995; Field Museum, Grant/Award Number: Brown Graduate Fellowship; University of Chicago, Grant/Award Number: Henry Hinds Fund

Abstract

Several prominent evolutionary theories propose mechanisms whereby the evolution of a defensive trait or suite of traits causes significant shifts in species diversification rate and niche evolution. We investigate the role of cuticular spines, a highly variable morphological defensive trait in the hyperdiverse ant genus *Polyrhachis*, on species diversification and geographic range size. Informed by key innovation theory and the escape-and-radiate hypothesis, we predicted that clades with longer spines would exhibit elevated rates of diversification and larger range sizes compared to clades with shorter spines. To address these predictions, we estimated phylogenetic relationships with a phylogenomic approach utilizing ultraconserved elements and compiled morphological and biogeographic trait databases. In contrast to the first prediction, we found no association between diversification rate and any trait (spine length, body size and range size), with the sole exception of a positive association between range size and diversification in one of three trait-based diversification analyses. However, we recovered a positive phylogenetic correlation between spine length and geographic range size, suggesting that spines promote expanded geographic range. Notably, these results were consistent across analyses using different phylogenetic inference approaches and spine trait measurement schemes. This study provides a rare investigation of the role of a defensive trait on geographic range size, and ultimately supports the hypothesis that defensive spines are a factor in increased range size in *Polyrhachis* ants. Furthermore, the lack of support for an association between spines and diversification, which contrasts with previous work demonstrating a positive association between spines and diversification rate, is intriguing and warrants further study.

KEYWORDS
defensive trait, geographic range size, morphology, trait-based diversification, ultraconserved elements

INTRODUCTION

Defensive traits can play a key role in the evolution of a clade, promoting coevolutionary dynamics with predators (Brodersen et al., 2018; Edger et al., 2015), geographic range size contractions or expansions (Luiz et al., 2013; Siemens et al., 2009), niche specialization (Darst et al., 2005) and morphological divergence (Kursar et al., 2009; Vamosi & Schluter, 2004). Prominent evolutionary theories propose putative mechanisms whereby the evolution of a defensive trait or suite of traits results in significant shifts in species diversification rate and niche evolution. One such theory proposes that the evolution of a 'key innovation' drives subsequent significant increases in diversification rates (Mayr, 1960), for example, the association between the evolution of extrafloral nectaries, an ant-mediated

FIGURE 1 Morphological variation in the ant genus *Polyrhachis*. Species (and photo credit), from top left: *P. boltoni* (Michael Esposito), *P. robsoni* (Will Ericson), *P. deceptor* (April Noble), *P. loweryi* (Will Ericson), *P. ornata* (Michele Esposito), *P. lata* (Cerise Chen), *P. hippomanes* (April Noble), *P. armata* (Estella Ortega) and *P. ypsilon* (Estella Ortega). Images from www.antweb.org under a Creative Commons attribution licence (accessed 13 June 2019). Figure reproduced from Blanchard et al. (2020) under a Creative Commons CC BY licence.

defence and elevated diversification in vascular plants (Weber & Agrawal, 2014). Similarly, the escape-and-radiate hypothesis proposes that escape from predators, deriving from the evolution of some defensive trait, drives cycles of diversification (Ehrlich & Raven, 1964). While the plant-butterfly herbivore system is the paradigmatic test case for this hypothesis (Suchan & Alvarez, 2015), Arbuckle and Speed (2015) find support for elevated speciation rates in frog clades that utilize aposematic coloration. Evaluating the influence of morphological defensive traits on macroevolutionary dynamics typically requires robust phylogenetic information and a clade that is diverse enough to include many phylogenetically independent evolutionary shifts in the traits of interest (Maddison & Fitz John, 2015).

The spiny ant genus *Polyrhachis*, a hyperdiverse clade of 700 described species and 82 valid subspecies (Bolton, 2020) with a broad geographic range spanning from western Africa to Melanesia, exhibits remarkable interspecific variation in cuticular spine morphology. Spine trait states range from entirely absent to extreme lengths exceeding that of the thorax (Figure 1), while species exhibit minimal intraspecific variation within the monomorphic worker caste. Recent work has established that such spines are likely adaptive defences against vertebrate and invertebrate predation (Blanchard et al., 2020; Ito et al., 2016; Pekár et al., 2017), with one study finding support for a muscle storage function of pronotal spines in the hyperdiverse ant genus *Pheidole* (Sarnat et al., 2017). Furthermore, a broad investigation across all ants found that spines are highly evolutionary labile and associated with elevated diversification rates (Blanchard & Moreau, 2017). *Polyrhachis* species also vary wildly in their geographic range even within the same subgenus, with some species restricted to one locality while others are distributed across much of the Oriental and Australasian regions (AntMaps.org; Guénard et al., 2017; Janicki et al., 2016). This insect genus is thus ideal for probing the relationship between a variable defensive trait and species diversification as well as geographic range size.

Ant phylogenetics has expanded into the field of phylogenomics through the use of RADseq (Fischer et al., 2015; Moreau & Wray, 2017), genotyping by sequencing (Winston et al., 2017), transcriptomics (Johnson et al., 2013) and, most recently, ultraconserved elements (UCEs; Branstetter, Longino, et al., 2017; Faircloth et al., 2012; Zhang et al., 2019). The use of UCEs has proven fruitful

in ants and other animal groups, contributing to the phylogenetic resolution of Hymenoptera (Branstetter, Danforth, et al., 2017), Formicidae (Branstetter, Longino, et al., 2017), and major ant lineages like Formicinae (Blaimer et al., 2015) and fungus-farming ants (Branstetter, Ješovnik, et al., 2017; Ješovnik et al., 2017), in addition to weevils (Van Dam et al., 2017), placental mammals (McCormack et al., 2012), ray-finned fishes (Faircloth et al., 2013), turtles (Crawford et al., 2015) and several other taxa (Zhang et al., 2019).

Here, we leverage the UCE sequencing approach to significantly expand the current phylogenetic coverage of *Polyrhachis* (Mezger & Moreau, 2016) and compile a dataset including spine length, body size, and range size information. With these data, we explore the impact of spine length evolution on species diversification and geographic range size while also accounting for body size, with a focus on expectations of defensive trait-based theories such as the escape-and-radiate hypothesis. In particular, we predicted that spines would be associated with both elevated diversification rates and expanded geographic range size, as expected if spines serve as defensive mechanisms that reduce extinction rates and promote spatial niche expansion due to a reduction of worker loss from predation.

MATERIALS AND METHODS

Taxon sampling

Our dataset for UCE sequencing includes 161 samples from 160 species, representing 12 of the 13 recognized subgenera and spanning the geographic range of the genus (sequencing failed for the representative of the species-poor *P. [Hirtomyrma]* subgenus; Table S1). We obtained samples from specimens collected for a previous study (Mezger & Moreau, 2016), gifts and loans from collaborators and the personal collections of authors of this study (B.D.B. and C.S.M.). Species were determined by B.D.B. using primary literature (Kohout, 2010; Kohout, 2014; Rigato, 2016), existing designations from Mezger and Moreau (2016) and information and images available on AntWiki (antwiki.org; accessed September 2018) and AntWeb (antweb.org; accessed September 2018). Any specimens identified to subspecies were treated as the parent species. See Table S2 for available collection information for each sample as well as voucher identity and depository location.

UCE sequencing workflow and bioinformatics

We conducted DNA extraction using the Qiagen DNEasy Blood and Tissue Kit (Qiagen Inc., Valencia, CA, USA) following the protocol of Moreau (2014). After this step, library preparation, sample pooling, UCE enrichment (Hymenoptera version 2 'ant specific' bait set targeting 2524 UCE loci; Branstetter, Longino, et al., 2017), enrichment verification, final pooling and Illumina sequencing followed the protocols described in Faircloth et al. (2015) (Appendix S1). All steps except Illumina sequencing were conducted in the Field Museum Pritzker Laboratory, after which sample pools were sent to the University of Oregon GC3F iLab for Illumina sequencing on an Illumina HiSeq 4000 (150 bp paired-end reads; Illumina Inc., San Diego, CA, USA; see Table S2 for NCBI accession numbers associated with raw demultiplexed sequences generated for this study). For a few samples from a previous study (Mezger & Moreau, 2016), extracted DNA was already available, and thus we skipped the extraction step. We selected 15 taxa to use as outgroups from a previous phylogenomic study that utilized an earlier probe set targeting 1510 UCE loci (Blaimer et al., 2015; Faircloth et al., 2015; Table S1), downloaded FASTQ files of trimmed reads through the Sequence Read Archive (Leinonen et al., 2011), and used these data in subsequent steps. All processing steps, from cleaning to alignment, were conducted using PHYLUCE v1.6.6 (Faircloth, 2016) on the University of Chicago Research Computing Center Midway2 computing cluster (see Appendix S1).

Phylogenomic analyses of 70% taxon complete matrix

Using the 70%-taxon-complete dataset, we inferred phylogenetic tree topologies through maximum likelihood (ML), Bayesian inference (BI) and gene-tree (GT) methods. For the ML analysis, we conducted inferences using RAxML-HPC BlackBox (Stamatakis, 2014) on the CIPRES computing cluster (Miller et al., 2010), enabling the AutoMRE function to allow the program to automatically determine sufficient bootstrapping number. We also designated all 15 outgroup taxa as outgroups, without constraining outgroup topology a priori, in the RAxML analysis. We conducted ML analyses using three partitioning schemes on the concatenated dataset: unpartitioned, locus-partitioned (partitioned by UCE locus) and rclusterf-partitioned using PartitionFinder2 with UCE loci as input data blocks (475 partitions; Lanfear et al., 2017). We used the GTR+ Γ model of molecular evolution for all inferences including the rclusterf-partitioned analysis. The rclusterf partitioning scheme was favoured by Akaike information criterion (AICc) analysis, thus we used the rclusterf-partitioned RAxML tree for downstream analyses.

For the BI analyses, we conducted an inference using the rclusterf-partitioned matrix in ExaBayes v1.5 (Aberer et al., 2014) on the CIPRES computing cluster. We conducted two runs with 1 million generations, a checkpoint interval of 10,000, four coupled chains and a 10% burn-in, with all other settings left at the default. We confirmed convergence and adequate effective sample size (ESS) values of both runs combined using Tracer v1.7.1 (Rambaut et al., 2018). We also enabled the 'consense' function to produce an output consensus tree with a threshold of 50% and a burn-in of 10%.

We conducted GT analyses using IQ-TREE v1.6.12 (Nguyen et al., 2015) and ASTRAL-III v5.6.3 (Zhang et al., 2018) on the Midway2 computing cluster. We implemented fast ML inferences in IQ-TREE for each UCE locus, utilizing the default 'ModelFinder' function that automatically selects the substitution model and including 1000 bootstraps, and exported the inferred tree, with labelled bootstrap support, for each locus. Previous work has shown that statistically binning loci into clusters can reduce error from loci with low information

content (Branstetter, Danforth, et al., 2017), and thus we implemented the statistical binning pipeline (Mirarab et al., 2014). However, the binning method failed to bin genes together, even with a threshold set to 90%, due to the presence of highly supported conflicts (S. Mirarab, personal communication), so we proceeded without binning UCE loci. We ran ASTRAL-III on our ML tree set using local posterior probability to assess node support, after collapsing branches with <10% support to improve accuracy (Zhang et al., 2017) using Newick Utilities v1.6 (Junier & Zdobnov, 2010).

Divergence dating

We implemented divergence dating analyses using our rclusterf-partitioned RAxML tree in MCMCTree, which is part of PAML v4.9 e (Yang, 2007), as well as BEAST2 (Bouckaert et al., 2019). We chose the RAxML topology (which is identical to the ExaBayes topology) as input, because the ASTRAL-III topology included a highly unusual placement for an in-group taxon (see Results). Due to current computational limitations, phylogenomic studies are limited to a small subset of the entire available data matrix when conducting divergence dating in BEAST2 (Bouckaert et al., 2019). We chose MCMCTree as an alternative because it is a more efficient program and also now has a sister R package, MCMCtreeR (Puttick, 2019), for setting and visualizing intuitive node priors, a former limitation. Furthermore, we used the 'approximate likelihood' method in MCMCTree to calculate the likelihood function during MCMC iteration (Reis & Yang, 2011), allowing the use of all 1300 UCE loci in our 70% taxon-complete dataset. For our BEAST2 runs, we used two different subsets of 100 UCE loci in our UCE dataset: '100-Random' (100 random loci) and '100-BEST' (100 loci with highest gene tree bootstrap support). Due to a lack of informative fossils for this group (the only fossil species *Polyrhachis annosa* is from a Late Miocene deposit much younger than both crown *Polyrhachis* and the subgenus to which it is tentatively assigned, *P.* [*Myrmatopa*]; Wappler et al., 2009), we set node age priors on outgroup nodes and the *Polyrhachis* crown node based on means and confidence intervals from previous phylogenetic studies (Table S3; see Results for some more details about outgroup noncongruence with previous studies). See Appendix S1 for further details and parameter settings implemented for our MCMCTree and BEAST2 inferences.

We used the posterior tree with RAxML-inferred topology and mean node ages from the 95% height posterior density (HPD) distribution inferred in MCMCTree for downstream macroevolutionary analyses. From the BEAST2 runs, as the 100-BEST and 100-RANDOM dataset analyses inferred extremely similar divergence dates (see Results) and the 100-BEST runs produced generally higher ESS values, we used only the 100-BEST MCC tree from the combined three independent runs for downstream macroevolutionary analyses.

Trait database

We collected morphological and geographic range trait data for the 160 *Polyrhachis* species included in our dated MCMCTree and BEAST2 phylogenies. To obtain linear measurements of worker body size and total spine length, we downloaded up to three available image sets from AntWeb (antweb.org; accessed December 2019) and AntWiki (antwiki.org; accessed December 2019), where each image set includes one lateral view and one dorsal view for a sample. Images were available for nearly all species, including 81 species (50.6%) with three image sets or more, 46 species (28.8%) with two image sets and 27 species (16.9%) with 1 image set, while only 6 species (3.8%) had no image sets available. From these images, we conducted linear measurements in ImageJ v2.0.0 (Rueden et al., 2017; Schindelin et al., 2012). To capture the *body size* metric, we used Weber's length, a standard proxy metric of body size used in ants (diagonal length of the mesosoma in lateral view; Figure S1). To capture total spine length (*spine length*), as we were interested in overall tissue investment in spine production, we measured the linear distance in millimetres from the base of a spine to the tip, for one of each pair of spines present on the pronotum, mesonotum, propodeum and petiole, and summed these values together. For each spine in a sample, we used the image orientation (lateral or dorsal) that was most parallel to the plane of projection of the spine. For a few cases, a singular spine—or spine triplet—was present (e.g. in *P.* [*Myrmothrinax*] spp.) rather than a typical pair of spines. In this situation, we included half the length of the solitary spine in our total spine length measurement (Table S1) in order to correspond to our measurement of spine pairs, which only includes one (i.e., 50%) of the total spine production for that pair. For curved spines, we used the 'segmented line' tool to measure linear length along the curvature of the spine. See Figure S1 for examples of different spine measurements. As an alternative metric of spines, we created a *max spine length* variable generated by using only the single longest spine measurement on any segment out of all measurements of the pronotal, mesonatal, propodeal and petiolar spines for each species. We also used *relative spine length* and *relative max spine length* (*spine length/body size* and *max spine length/body size*, respectively) for some analyses. Measurements for species with multiple image sets were averaged together.

We collected geographic range data from two sources. We used AntMaps.org (Guénard et al., 2017; Janicki et al., 2016), an online database of ant distribution records, to record presence/absence of each of the 160 species in our dataset within three large biogeographic categories, Afrotropical, Oriental and Australasian (Lomolino et al., 2005; Mezger & Moreau, 2016), using Wallace's line (Wallace, 1863) to separate Oriental from Australasian. For a more fine-grained dataset, we utilized the recently published global ant distribution data of Kass et al. (2022), extracting geographic ranges in TIF file format derived from either polygons based on alpha hulls or buffered points (depending on number of collections available; see Kass et al., 2022, for more details). We imported each TIF file into QGIS v3.22.10 (QGIS.org, 2020), implemented the *Polygonize* function with default settings to convert the raster into a polygon, calculated the total spatial area in square metres using the *area* function in the attribute table, and converted this number to square kilometres. We used these area data as the *range size* data for the 154 species from which we could collect morphological data.

Macroevolutionary analyses

For all macroevolutionary analyses, we used both the MCMCTree and BEAST2-100BEST time-scaled phylogenies. We inferred ancestral states along each phylogeny for *relative spine length*, *relative max spine length*, *body size* and *range size* using the *contMap* function in phytools v0.6 (Revell, 2012, 2013) implemented in RStudio v1.2.5033 (R Core Team, 2018; RStudio Team, 2015). We also inferred ancestral geographic ranges using BioGeoBEARS v1.1.2 (Matzke, 2013). We utilized the DEC, BAYAREALIKE and DIVALIKE models without the jump dispersal/founder-event speciation parameter (J), given the very large size of our three biogeographic regions (designated as three areas in the analyses with a max range size of three areas) and concerns pertaining to the 'jump' parameter (Ree & Sanmartín, 2018), and selected the model with the best fit according to Akaike information criterion (AIC).

We conducted diversification analyses using several methods. To assess shifts in diversification independent of a priori trait information, we used BAMM v2.5.0 and BAMMtools v2.1.7 (Rabosky, 2014; Rabosky et al., 2014). We enabled the *sampleProbsFilename* option to account for differing levels of taxon sampling across the 12 *Polyrhachis* subgenera included in our phylogeny, with sampling estimates based on current subgeneric taxonomy as determined from AntWiki (antwiki.org; accessed September 2018) and a backbone sampling probability of 0.986 to account for the missing 10 species from the unsampled *P.* (*Hirtomyrma*) subgenus. For cases of inferred polyphyletic subgenera, we applied the sampling fraction for the subgenus to each independent clade. We set values for the *expectedNumberOfShifts*, *lambdaInitPrior*, *lambdaShiftPrior* and *muInitPrior* priors using the *setBAMMpriors* function in BAMMtools, which is designed to select appropriate priors based on features of the input dataset. With all other settings left at the default, we ran the MCMC for 10 million generations, sampling every 10,000 generations, and assessed convergence in BAMMtools, with a burn-in of 15%, to ensure that the effective size of the estimated number of shifts and log likelihood each exceeded 100. We then evaluated the event data using BAMMtools, to assess the inferred average phylorate across the *Polyrhachis* phylogeny, as well as the 95% credible set of distinct shift configurations (i.e., the set of distinct shift configurations that account for 95% of the probability of the data).

To assess evidence for trait-based diversification, we implemented an analysis in QuaSSE (Fitz John, 2010) in the package diversitree v09-13 (Fitz John, 2012). For each trait, we used the *starting.point.quasse* function to set starting points for each model based on parameters estimated using birth-death and Brownian motion models of evolution. We then used an analysis of variance to compare the fit of a trait-correlated versus trait-uncorrelated model of diversification. Due to documented type 1 error issues with the state speciation and extinction (SSE) suite of models under some scenarios (Rabosky & Goldberg, 2015), we also used *ES-sim* v1.1 (Harvey & Rabosky, 2018), which tests for correlations between summary statistics of phylogenetic branching patterns and trait variation at the tips of a phylogeny and is designed as an alternative to QuaSSE. We ran 1000 simulations in *ES-sim* for each trait.

Finally, to test for correlations between spine length, body size, and range size, we conducted a phylogenetic generalized least squares (PGLS) analysis in the R package caper v1.0.1 (Orme et al., 2018). One of our predictions was that spine length should promote, and thus be positively correlated with, increased geographic range size, thus we set *range size* as the response variable and included both *spine length* (or *max spine length*) and *body size* as factors. We also tested for a correlation between *body size* and *spine length* (or *max spine length*) to test for potential allometric scaling between spine length and body size. For all PGLS analyses, variables were log-transformed prior to analysis (Mundry, 2014), and we optimized the three branch length transformations—lambda, delta and kappa – using caper's ML setting.

RESULTS

UCE capture statistics

Our 70% taxon complete matrix includes 161 samples from 160 *Polyrhachis* species, representing approximately 23% of the hyperdiverse genus (Bolton, 2020), and 15 outgroup Formicine taxa. The raw sequence data consisted of a mean of 7.2 million reads per sample with a mean length of 140 bp (Table S4). The Trinity assembly step resulted in a mean of 98,505 contigs with a mean length of 377.7 bp and mean coverage of 5.7X. After the finding UCE loci step, we recovered a mean of 1653 UCE contigs per sample, with a mean contig length of 865 bp and a mean coverage per UCE of 31.38X (Table S4). The final matrix of concatenated UCE loci was 592,434 bp long and included 1300 UCE loci alignments and 105,976 informative sites (with 4.9% missing data, including gaps).

Phylogenomic analyses

Our PartitionFinder2 analyses, using the rclusterf algorithm, produced a partitioning scheme with 475 subsets. The rclusterf-partitioned dataset was favoured via AICc analysis, although the mean branch support, tree length, mean branch length and branch length variance were relatively similar for all partitioning schemes (Table S5), suggesting minimal impacts of partitioning scheme.

The final tree topologies for our ML, BI and GT analyses were largely consistent with each other. The ML and BI topologies were identical to each other, with only some differences in bootstrap versus posterior probability node support (Figures 2, S2, and S3, Appendix S1). The GT topology was similar to that of the ML and BI trees at the subgeneric level, with some exceptions at the species level (Figure S4). The most unusual incongruity in the GT inference is the placement of *P. lamellidens*, a well-supported member of the highly distinct *P.* (*Polyrhachis*) subgenus. In the GT topology, this species is placed away from the *P.* (*Polyrhachis*) subgenus and instead sister to the entire *Polyrhachis-Myrma* clade, possibly due to lower locus coverage for this taxon (414 loci) resulting in its absence from too many gene trees to be accurately placed in the species tree. This major

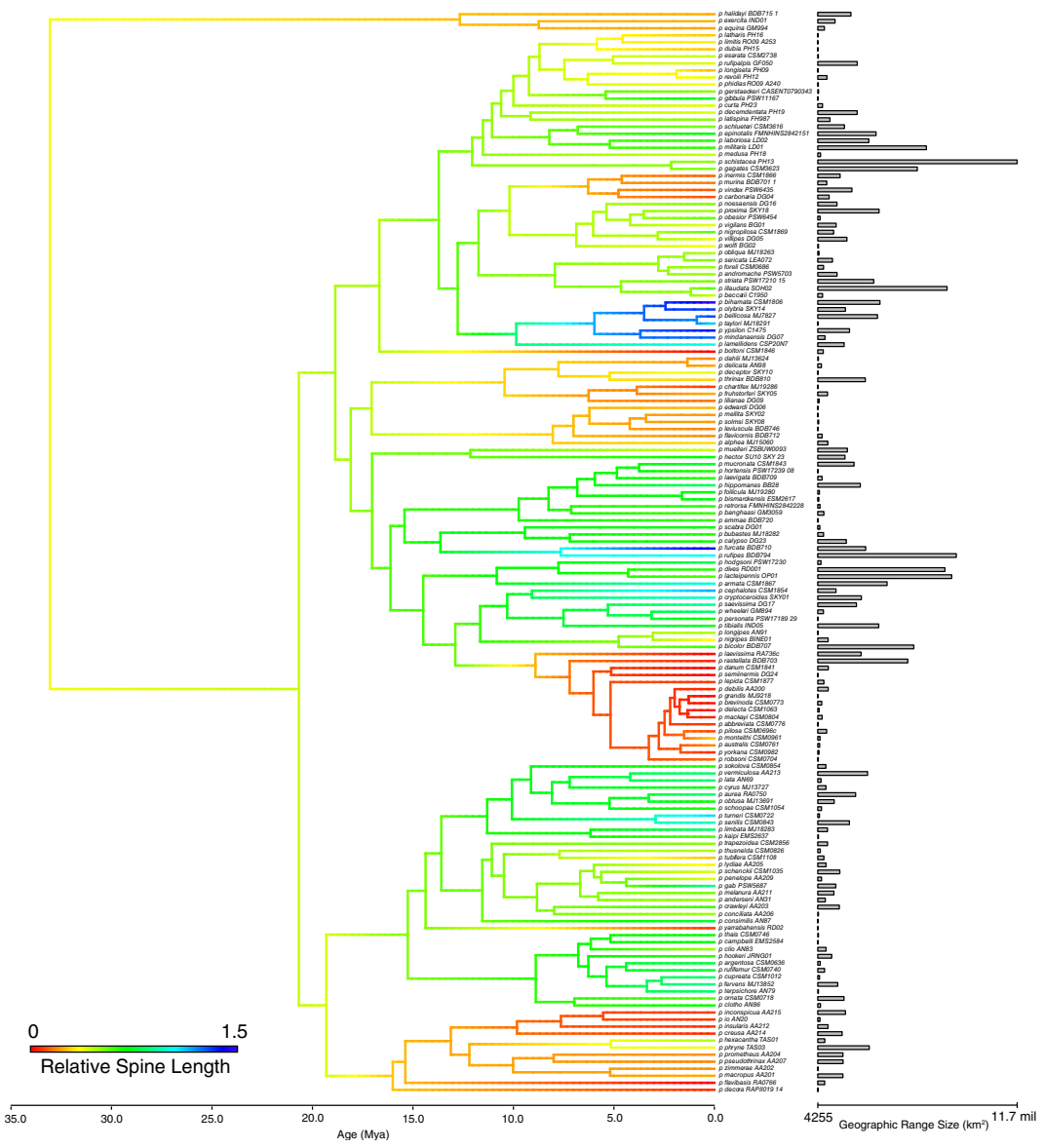

FIGURE 2 MCMCTree time-scaled phylogeny inferred with RAxML topology. Bars display geographic range size for each species, and the ancestral state reconstruction of *relative spine length* is mapped along the phylogeny.

inconsistency led us to favour the ML/BI topology, which we used for divergence dating. The subgeneric relationships found in our ML/BI tree topology are also broadly similar to the relationships reported in the seven gene-based phylogeny of Mezger and Moreau (2016), with a couple notable exceptions (see Appendix S1 for more discussion on comparisons between these two studies). Overall, the consistency of our trees across differing phylogenetic inference methods, and similarities with Mezger and Moreau (2016), supports the robustness of our topological inference, with the gene-tree method producing the most divergent results.

Divergence dating in MCMCTree using our rclusterf-partitioned RAxML starting tree reconstructed a node age for crown *Polyrhachis* of 33 Ma (95% HPD: 21.16–48.73 Ma), a slightly younger age compared to the previous molecular phylogenetic study of the genus that inferred a crown age of 42 Ma (Mezger & Moreau, 2016). Importantly, the outgroup relationships are not resolved with respect to *Polyrhachis*, likely a consequence of reduced taxon sampling of the outgroups relative to their source study (Blaimer et al., 2015), which itself included uncertainty around the placement of *Oecophylla*, *Gesomyrmex* and *Myrmoteras*. This sparse sampling likely perturbed the inferred topology of the outgroups in our RAxML and ExaBayes inferences. This circumstance could have impacted our inference of the crown age of *Polyrhachis*. However, *Polyrhachis* is well-established as a monophyletic genus (Blaimer et al., 2015; Mezger & Moreau, 2016; Moreau & Bell, 2013), and our inferred age of the crown Formicinae subfamily, 126 Ma (95% HPD: 111.5–138.76 Ma), is consistent with the previous phylogenomic study of Formicinae (Blaimer et al., 2015) while older than the age inferred by two family-wide phylogenetic studies of the ants (Moreau & Bell, 2013; Nelsen et al., 2018). Furthermore, divergence dating in BEAST2 reconstructed a crown node age of 52 Ma with the 100-BEST dataset and 51 Ma with the

100-RANDOM dataset, thus inferring an older (rather than younger) age compared to the previous *Polyrhachis* study, while also inferring a crown age of Formicinae of 128 Ma that is comparable to the prior Formicinae study. It therefore does not appear that outgroup inferences uniformly significantly bias our divergence dating inferences.

Diagnostic priors-only runs in MCMCTree established that our data substantially impact both inferred node dates and estimated relative branch lengths between subclades under the independent rates model (Figures S5–S7) but not the correlated rates model (Figures S8–S10). We also found significant impacts of molecular data on the posterior distribution of ages inferred in our BEAST2 runs (Figures S11–S13). Outgroups were pruned for subsequent analyses using our time-scaled MCMCTree and BEAST2 phylogenies. As the inferred divergence dates for the 100-BEST and 100-RANDOM datasets were highly similar, we used the BEAST2-100BEST phylogeny as an older estimate of *Polyrhachis* divergence dates, and the MCMCTree phylogeny as a younger estimate, for downstream macroevolutionary analyses.

Macroevolutionary analyses

Our database includes morphological trait data for 154 of the 160 *Polyrhachis* species in our 161-tip time-scaled phylogenies (Table S1). In addition to outgroups, we pruned the six taxa without morphological information as well as one of the two *P. armata* tips to ensure even sampling of species included in our MCMCTree and BEAST2 trees. These two 154-tip *Polyrhachis* phylogenies were used for all macroevolutionary analyses.

Ancestral state estimation analyses demonstrate wide variation in *relative spine length*, *body size* and *range size*, with multiple phylogenetically independent gains and losses of trait states for all of these traits (Figures 2 and S14–S17). Very long relative spine lengths are inferred to have evolved independently at least five times, while very small spines—or complete spine loss—has independently occurred at least seven times (Figures S14 and S15). Large body size appears to have evolved at least 10 times and small body size at least 5 times (Figure S16). One portion of the *Polyrhachis* phylogeny exhibits consistently small range size (species found in approximately one to three regions), whereas the rest of the tree is more variable, including at least three independent gains of very large range size (Figure S17).

Our BioGeoBEARS analysis selected BAYAREALIKE as the best-fitting model (ΔAIC > 19.9 relative to both other models). As in Mezger and Moreau (2016), a joint Oriental/Australasian origin is inferred as the ancestral state of crown *Polyrhachis*, consistent with a Southeast Asian origin of the genus (Figures S18 and S19). Relative to our ancestral range estimation results based on three broad biogeographic categories, our finer-scale range size data reveals fairly high evolutionary lability of range size, with sizes ranging from a small

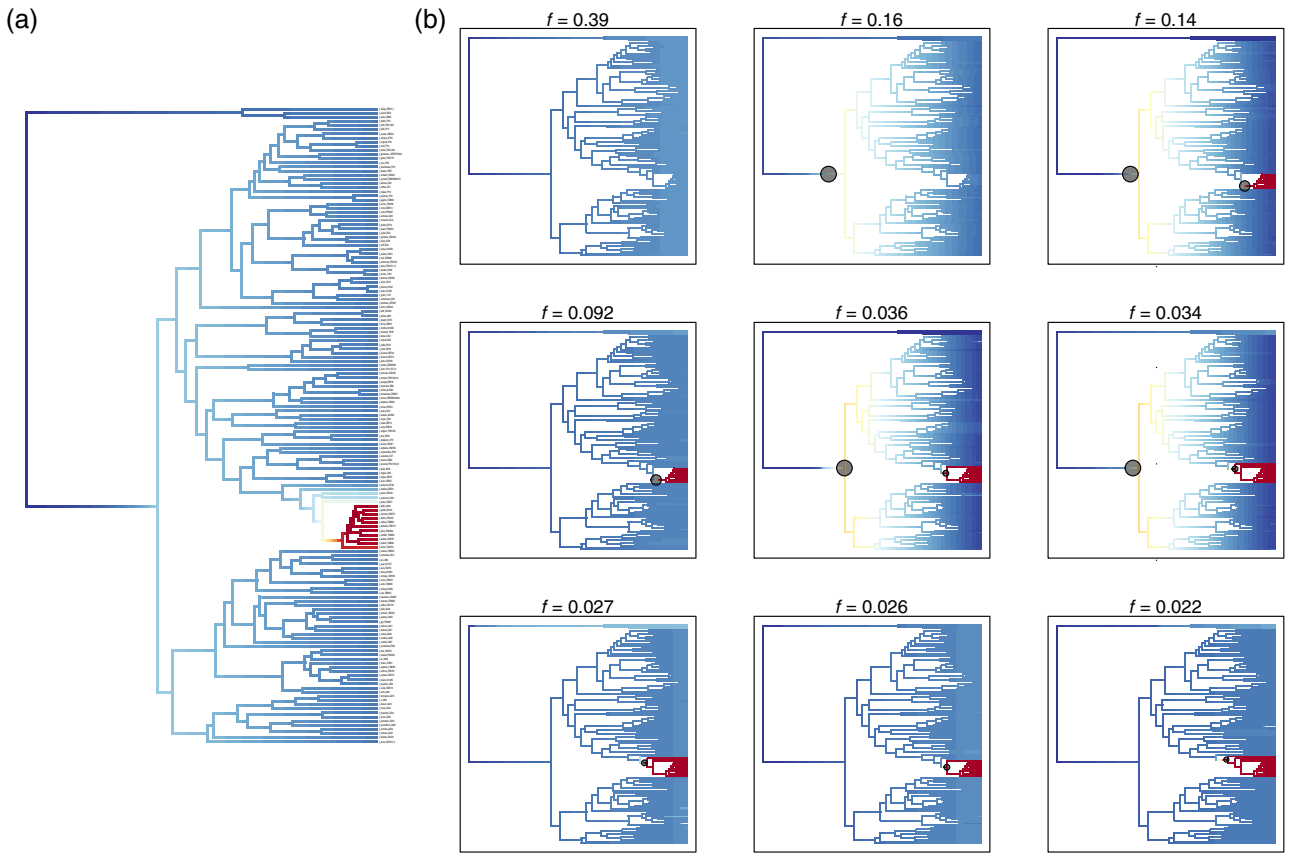

FIGURE 3 Results from a BAMM analysis of the time-scaled MCMCTree phylogeny. (a) Mean phylorate plot. (b) 95% credible shift set (nine plots representing 0.927 frequency displayed).

distribution of about 4000 km^2 up to very large distribution exceeding 11 million km^2 (Figures 2 and S17).

Diversification analyses, implemented using three different methods and phylogenies inferred through two different methodological approaches, consistently found no association between diversification rate and any of our traits (*spine length*, *maximum spine length*, *body size* and *range size*). With our MCMCTree phylogeny, our BAMM analyses produce average phylorate plots with an apparent rate increase in the *Cyrtomyrma* subgenus, which is notable for a nearly complete lack of spines, but the majority of configurations in the 95% credible shift set (0.55 frequency) lack an inferred rate shift in the subgenus (Figure 3). Furthermore, the single most frequent configuration (0.39 frequency) infers zero rate shifts. In *ES-sim*, we recovered no association between diversification and *spine length* ($p = 0.829$), *maximum spine length* ($p = 0.845$), *relative spine length* ($p = 0.759$), *relative maximum spine length* ($p = 0.823$), *body size* ($p = 0.454$) or *range size* ($p = 0.524$) (Table S6). Similarly, our QuaSSE analyses did not support a trait-dependent model of diversification when compared to a trait-independent model, for any trait ($p > 0.376$ for all six traits; Table S6). All these results are qualitatively identical to the results using the BEAST2-100BEST phylogeny (Figure S20, Table S6), with the single exception of a statistically significant positive association between *range size* and diversification in QuaSSE ($p < 0.001$; Table S6).

PGLS analyses revealed some evolutionary correlations between our log-transformed traits. In particular, we found a significant positive association between *spine length* and *range size* ($p = 0.025$, $R^2 = 0.036$), while finding that *body size* is not associated with *range*

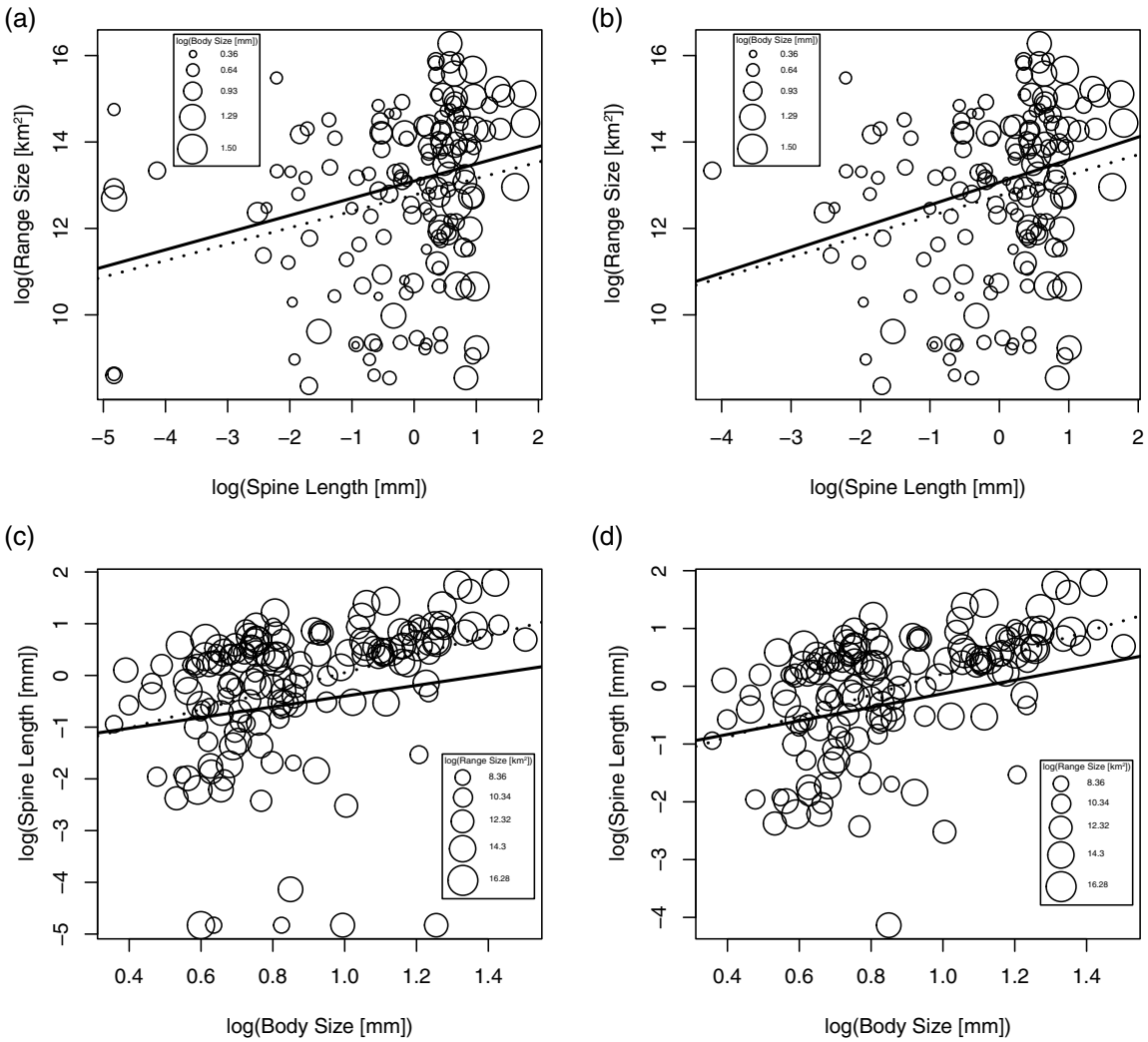

FIGURE 4 Phylogenetic generalized least squares (PGLS) analyses including *spine length*, *body size* and *range size*. Panels (a) and (b) display results from a bivariate PGLS model including *spine length* as a predictor of *range size*, with and without zero-spine taxa included, respectively. Point size corresponds to *body size*. Panels (c) and (d) display results from a bivariate PGLS model including *body size* as a predictor of *spine length*, with and without zero-spine taxa included, respectively. Point size corresponds to *range size*. In panels (a) to (d), the solid trend line corresponds to the bivariate PGLS analysis, and the dotted trend line corresponds to a bivariate standard regression conducted using the 'lm' function in R. The values for all variables have been log-transformed. See Table S7 for full results from the multivariate PGLS analyses including both *spine length* and *body size* as predictors of *range size*.

size ($p = 0.378$) (Figure 4, Table S7). *Spine length* also positively scales with *body size* ($p < 0.001$, $R^2 = 0.055$), without clear evidence of allometric scaling (Figure 4, Table S7). These results did not significantly differ when using *maximum spine length* as an alternative spine metric or with zero-spine taxa excluded, although *maximum spine length* was only marginally significantly associated with *range size* when zero-spine taxa were excluded ($p = 0.064$; Table S7). As with the diversification analyses, these results also did not qualitatively differ from those using the BEAST2-100BEST phylogeny (Table S7).

DISCUSSION

We reconstructed a large phylogeny of the hyperdiverse spiny ant genus *Polyrhachis* using a phylogenomic UCE approach, resulting in robust time-scaled trees inferred by two different methods that include 160 species from 12 of the 13 recognized subgenera in the genus. Using these phylogenies and our compiled database of spine length, body size and geographic range size data, we found a positive correlation between spine length and geographic range (Figures 2 and 4, Table S7). Although the R^2 value is low, this result supports the hypothesis that spines contribute to broader geographic range sizes in *Polyrhachis*, potentially due to a reduction in worker loss from predation. Interestingly, our results also consistently support no association between spine length and diversification, regardless of analysis or phylogeny used (Figure 3, Table S6), in contrast to our expectation that spines should promote elevated diversification rates.

While we find a positive association between defensive traits and geographic range, some studies in plants find the reverse: defence specialization adapted to local enemies restricts geographic range and/or constrains range evolution (Agrawal et al., 2005; Siemens et al., 2009). Our alternative result may arise from the fact that ant spines should serve as quite generalized and energetically cheap defences against most myrmecophagous predators, and consequently do not carry the spatially constraining costs associated with specialization. Thus, similar to invasive species experiencing enemy release that facilitates invasion into novel environments (Keane & Crawley, 2002), long spines in *Polyrhachis* workers may afford escape from widespread predators—such as frogs (Ito et al., 2016) and spiders (Blanchard et al., 2020)—regardless of geographic location. Direct tests of a defensive trait-geographic range size relationship are surprisingly rare, but Luiz et al. (2013) present a similar case in tropical reef fishes, where adult defensive traits (schooling behaviour and nocturnal activity) predicted larger geographic range size.

One potential confounding effect in such studies, including ours, is that more conspicuous species may be disproportionately collected relative to less conspicuous species, potentially influencing range size comparisons. Future work in ants, as well as other taxa, should address the role of defensive traits on geographic range size as well as develop strategies to address collection bias. Additionally, such studies could jointly consider other factors known to impact geographic range size, including competition (Pigot & Tobias, 2013) and dispersal ability (Capurucho et al., 2020). It is also notable that Sarnat et al. (2017) found that all six extant lineages that independently evolved spines in the nearly global genus *Pheidole* are restricted to the Asia-Pacific region, suggesting some unique evolutionary driver of spine evolution in this region that is the cradle of both *Polyrhachis* and *Pheidole* spiny ant diversification. Given evidence demonstrating an impact of geological history (e.g., land bridge formation: Price et al., 2022; Winston et al., 2017) and ecological opportunity (Economo et al., 2015; Price et al., 2014; Sarnat & Moreau, 2011) on ant evolutionary history, as well as newly available global ant trait and geographic range databases (Kass et al., 2022; Parr et al., 2017), the role of biogeographic factors on morphological trait evolution in ants should be further explored.

The lack of a relationship between spines and diversification within *Polyrhachis* is intriguing, as it contrasts with previous work across all ants at the taxonomic scale of the genus (Blanchard & Moreau, 2017). The discordance between these two studies could suggest that spine evolution increased initial diversification during the early stages of radiation in the genus, following an 'early-burst' model (Losos & Mahler, 2010), but did not consistently drive diversification across the timespan of *Polyrhachis* evolution and is thus not captured using the methods in this study. It is also possible that geographic range expansion in single species promotes increased gene flow (Bohonak, 1999), such that more spinescent clades speciate at slower rates than less spinescent clades. Some studies on bird evolution support this dynamic, where increased dispersal abilities suppress diversification rates (Claramunt et al., 2012; Weeks & Claramunt, 2014). Spine expression may also carry costs that are not detectable in this study but may negate any enhancement of diversification rate resulting from expanded geographic range size. Potential costs include restriction of nesting site location (Wilson, 1959), navigational challenges (especially for individuals with very long spines traversing complex microhabitats), and early-stage developmental challenges or limitations associated with spine production. Notably, while our phylogenetic inference represents twice as many described species as the previous *Polyrhachis* phylogeny (Mezger & Moreau, 2016), our tree still includes only about 23% of all described taxa in the genus. Furthermore, among the three diversification analyses, only BAMM was able to incorporate variable taxonomic sampling information (runs in QuaSSE utilizing the *sampling.f* function failed to converge), and even this correction is not a substitute for real data. Recent work has also highlighted the extent of challenges faced by such diversification studies to infer correct diversification histories (Louca & Pennell, 2020; Rabosky et al., 2017). Thus, although all three analyses, which are each fundamentally different in their approach, were concordant in failing to support spine-based diversification in *Polyrhachis* regardless of phylogeny used, further phylogenetic sampling is necessary to more robustly establish the relationship, if any, between cuticular spines and diversification in the spiny ants.

Overall, our study provides a rare investigation directly assessing the role of a defensive trait on geographic range size, and ultimately supports the hypothesis that defensive spines are a factor in increased range size in *Polyrhachis* ants. Additionally, neither spine length nor range size expansion appears to be associated with elevated

diversification rates, a dynamic that should be the focus of future research. Our work adds to the growing body of evidence that defensive traits—and especially spines—play a key role in the evolution of ants and may significantly contribute to the evolutionary persistence and global dominance of this hyperdiverse clade of insects.

AUTHOR CONTRIBUTIONS

Benjamin David Blanchard: Conceptualization (lead); data curation (lead); formal analysis (lead); funding acquisition (supporting); investigation (lead); methodology (lead); project administration (lead); resources (supporting); software (lead); validation (lead); visualization (lead); writing – original draft (lead); writing – review and editing (lead). **Corrie Saux Moreau:** Conceptualization (supporting); funding acquisition (lead); project administration (supporting); resources (lead); supervision (lead); writing – review and editing (supporting).

ACKNOWLEDGEMENTS

We express our gratitude to Destiny Reeves, Manuela Ramalho, Shauna Price and Bonnie Blaimer for UCE sequencing support, as well as Kevin Feldheim for Pritzker DNA Discovery Lab logistical assistance. We are also thankful to Cathy Pfister, Trevor Price, Graham Slater and three anonymous reviewers for feedback on earlier versions of this manuscript. We are grateful for the University of Chicago Research Computing Center maintaining the Midway2 computing cluster and providing troubleshooting support. This work would not be possible without specimen contributions from several colleagues—we deeply appreciate gifted and loaned specimens for DNA extraction contributed by Alan Andersen, Francisco Hita Garcia, Benoit Guénard, Ben Hoffmann, Milan Janda, Matthew Prebus, Eli Sarnat and Phil Ward. We also appreciate data analysis assistance from Michael Branstetter, Brant Faircloth and Siavash Mirarab. This research was supported by National Science Foundation grants to Benjamin D. Blanchard and Corrie S. Moreau (DEB-1701352, IOS-1916995, DEB-1900357), as well as the Chinese Academy of Sciences Presidential International Fellowship Initiative grant number 2021PB0085, a grant from the University of Chicago Henry Hinds Fund for Evolutionary Research, and a Field Museum of Natural History Brown Graduate Fellowship, all awarded to Benjamin D. Blanchard.

CONFLICT OF INTEREST

The authors declare that there is no conflict of interest.

DATA AVAILABILITY STATEMENT

Raw demultiplexed sequence reads in FASTQ format are available from the NCBI Sequence Read Archive (see Table S2 for accession numbers). UCE contig files as well as all tree files, data, and scripts are deposited in the Dryad data repository (doi: https://doi.org/10.5061/dryad.ffbg79crt).

ORCID

Benjamin D. Blanchard https://orcid.org/0000-0002-7747-6934
Corrie S. Moreau https://orcid.org/0000-0003-1139-5792

REFERENCES

Aberer, A.J., Kobert, K. & Stamatakis, A. (2014) ExaBayes: massively parallel Bayesian tree inference for the whole-genome era. *Molecular Biology and Evolution*, 31, 2553–2556.

Agrawal, A.A., Kotanen, P.M., Mitchell, C.E., Power, A.G., Godsoe, W. & Klironomos, J. (2005) Enemy release? An experiment with congeneric plant pairs and diverse above-and belowground enemies. *Ecology*, 86, 2979–2989.

Arbuckle, K. & Speed, M.P. (2015) Antipredator defenses predict diversification rates. *Proceedings of the National Academy of Sciences*, 112, 13597–13602.

Blaimer, B.B., Brady, S.G., Schultz, T.R., Lloyd, M.W., Fisher, B.L. & Ward, P.S. (2015) Phylogenomic methods outperform traditional multi-locus approaches in resolving deep evolutionary history: a case study of formicine ants. *BMC Evolutionary Biology*, 15, 271.

Blanchard, B.D. & Moreau, C.S. (2017) Defensive traits exhibit an evolutionary trade-off and drive diversification in ants. *Evolution*, 71, 315–328.

Blanchard, B.D., Nakamura, A., Cao, M., Chen, S.T. & Moreau, C.S. (2020) Spine and dine: a key defensive trait promotes ecological success in spiny ants. *Ecology and Evolution*, 10, 5852–5863.

Bohonak, A.J. (1999) Dispersal, gene flow, and population structure. *Quarterly Review of Biology*, 74, 21–45.

Bolton, B. (2020) *An online catalog of the ants of the world*. Available at: http://www.antcat.org [Accessed February 2020]

Bouckaert, R., Vaughan, T.G., Barido-Sottani, J., Duchêne, S., Fourment, M., Gavryushkina, A. et al. (2019) BEAST 2.5: an advanced software platform for Bayesian evolutionary analysis. *PLoS Computational Biology*, 15, e1006650.

Branstetter, M.G., Danforth, B.N., Pitts, J.P., Faircloth, B.C., Ward, P.S., Buffington, M.L. et al. (2017) Phylogenomic insights into the evolution of stinging wasps and the origins of ants and bees. *Current Biology*, 27, 1019–1025.

Branstetter, M.G., Ješovnik, A., Sosa-Calvo, J., Lloyd, M.W., Faircloth, B.C., Brady, S.G. et al. (2017) Dry habitats were crucibles of domestication in the evolution of agriculture in ants. *Proceedings of the Royal Society B*, 284, 20170095.

Branstetter, M.G., Longino, J.T., Ward, P.S. & Faircloth, B.C. (2017) Enriching the ant tree of life: enhanced UCE bait set for genome-scale phylogenetics of ants and other Hymenoptera. *Methods in Ecology and Evolution*, 8, 768–776.

Brodersen, J., Post, D.M. & Seehausen, O. (2018) Upward adaptive radiation saccades: predator diversification induced by prey diversification. *Trends in Ecology & Evolution*, 33, 59–70.

Capurucho, J.M.G., Ashley, M.V., Tsuru, B.R., Cooper, J.C. & Bates, J.M. (2020) Dispersal ability correlates with range size in Amazonian habitat-restricted birds. *Proceedings of the Royal Society B*, 287, 20201450.

Claramunt, S., Derryberry, E.P., Remsen, J.V., Jr. & Brumfield, R.T. (2012) High dispersal ability inhibits speciation in a continental radiation of passerine birds. *Proceedings of the Royal Society B*, 279, 1567–1574.

Crawford, N.G., Parham, J.F., Sellas, A.B., Faircloth, B.C., Glenn, T.C., Papenfuss, T.J. et al. (2015) A phylogenomic analysis of turtles. *Molecular Phylogenetics and Evolution*, 83, 250–257.

Darst, C.R., Menéndez-Guerrero, P.A., Coloma, L.A. & Cannatella, D.C. (2005) Evolution of dietary specialization and chemical defense in poison frogs (Dendrobatidae): a comparative analysis. *The American Naturalist*, 165, 56–69.

Economo, E.P., Sarnat, E.M., Janda, M., Clouse, R., Klimov, P.B., Fischer, G. et al. (2015) Breaking out of biogeographical modules: range expansion and taxon cycles in the hyperdiverse ant genus *Pheidole*. *Journal of Biogeography*, 42, 2289–2301.

Edger, P.P., Heidel-Fischer, H.M., Bekaert, M., Rota, J., Glöckner, G., Platts, A.E. et al. (2015) The butterfly plant arms-race escalated by gene and genome duplications. *Proceedings of the National Academy of Sciences*, 112, 8362–8366.

Ehrlich, P.R. & Raven, P.H. (1964) Butterflies and plants: a study in coevolution. *Evolution*, 18, 586–608.
Faircloth, B.C. (2016) PHYLUCE is a software package for the analysis of conserved genomic loci. *Bioinformatics*, 32, 786–788.
Faircloth, B.C., Branstetter, M.G., White, N.D. & Brady, S.G. (2015) Target enrichment of ultraconserved elements from arthropods provides a genomic perspective on relationships among Hymenoptera. *Molecular Ecology Resources*, 15, 489–501.
Faircloth, B.C., McCormack, J.E., Crawford, N.G., Harvey, M.G., Brumfield, R.T. & Glenn, T.C. (2012) Ultraconserved elements anchor thousands of genetic markers spanning multiple evolutionary timescales. *Systematic Biology*, 61, 717–726.
Faircloth, B.C., Sorenson, L., Santini, F. & Alfaro, M.E. (2013) A phylogenomic perspective on the radiation of ray-finned fishes based upon targeted sequencing of ultraconserved elements (UCEs). *PLoS One*, 8, e65923.
Fischer, G., Azorsa, F., Garcia, F.H., Mikheyev, A.S. & Economo, E.P. (2015) Two new phragmotic ant species from Africa: morphology and next-generation sequencing solve a caste association problem in the genus *Carebara* Westwood. *ZooKeys*, 525, 77–105.
Fitz John, R.G. (2010) Quantitative traits and diversification. *Systematic Biology*, 59, 619–633.
Fitz John, R.G. (2012) Diversitree: comparative phylogenetic analyses of diversification in R. *Methods in Ecology and Evolution*, 3, 1084–1092.
Guénard, B., Weiser, M.D., Gomez, K., Narula, N. & Economo, E.P. (2017) The Global Ant Biodiversity Informatics (GABI) database: synthesizing data on the geographic distribution of ant species (Hymenoptera: Formicidae). *Myrmecological News*, 24, 83–89.
Harvey, M.G. & Rabosky, D.L. (2018) Continuous traits and speciation rates: alternatives to state-dependent diversification models. *Methods in Ecology and Evolution*, 9, 984–993.
Ito, F., Taniguchi, K. & Billen, J. (2016) Defensive function of petiole spines in queens and workers of the formicine ant *Polyrhachis lamellidens* (Hymenoptera: Formicidae) against an ant predator, the Japanese treefrog *Hyla japonica*. *Asian Myrmecology*, 8, 81–86.
Janicki, J., Narula, N., Ziegler, M., Guénard, B. & Economo, E.P. (2016) Visualizing and interacting with large-volume biodiversity data using client–server web-mapping applications: the design and implementation of antmaps.org. *Ecological Informatics*, 32, 185–193.
Ješovnik, A., Sosa-Calvo, J., Lloyd, M.W., Branstetter, M.G., Fernandez, F. & Schultz, T.R. (2017) Phylogenomic species delimitation and host-symbiont coevolution in the fungus-farming ant genus *Sericomyrmex* Mayr (Hymenoptera: Formicidae): ultraconserved elements (UCEs) resolve a recent radiation. *Systematic Entomology*, 42, 523–542.
Johnson, B.R., Borowiec, M.L., Chiu, J.C., Lee, E.K., Atallah, J. & Ward, P.S. (2013) Phylogenomics resolves evolutionary relationships among ants, bees, and wasps. *Current Biology*, 23, 2058–2062.
Junier, T. & Zdobnov, E.M. (2010) High-throughput phylogenetic tree processing in the UNIX shell. *Bioinformatics*, 26, 1669–1670.
Kass, J.M., Guénard, B., Dudley, K.L., Jenkins, C.N., Azuma, F., Fisher, B.L. et al. (2022) The global distribution of known and undiscovered ant biodiversity. *Science*. *Advances*, 8, eabp9908.
Keane, R.M. & Crawley, M.J. (2002) Exotic plant invasions and the enemy release hypothesis. *Trends in Ecology & Evolution*, 17, 164–170.
Kohout, R.J. (2010) A review of the Australian *Polyrhachis* ants of the subgenera *Myrmhopla* Forel and *Hirtomyrma* subgen. Nov. (Hymenoptera: Formicidae: Formicinae). *Memoirs of the Queensland Museum: Cultural Heritage Series*, 55, 167–204.
Kohout, R.J. (2014) A review of the subgenus *Polyrhachis* (*Polyrhachis*) Fr. Smith (Hymenoptera: Formicidae: Formicinae) with keys and description of a new species. *Asian Myrmecology*, 6, 1–31.
Kursar, T.A., Dexter, K.G., Lokvam, J., Pennington, R.T., Richardson, J.E., Weber, M.G. et al. (2009) The evolution of antiherbivore defenses and their contribution to species coexistence in the tropical tree genus *Inga*. *Proceedings of National Academy of the Sciences*, 106, 18073–18078.
Lanfear, R., Frandsen, P.B., Wright, A.M., Senfeld, T. & Calcott, B. (2017) Partition Finder 2: new methods for selecting partitioned models of evolution for molecular and morphological phylogenetic analyses. *Molecular Biology and Evolution*, 34, 772–773.
Leinonen, R., Sugawara, H., Shumway, M. & International Nucleotide Sequence Database Collaboration. (2011) The sequence read archive. *Nucleic Acids Research*, 39, D19–D21.
Lomolino, M.V., Riddle, B.R. & Brown, J.H. (2005) *Biogeography*. Sunderland, MA: Sinauer Associates, Inc.
Losos, J.B. & Mahler, D.L. (2010) Adaptive radiation: the interaction of ecological opportunity, adaptation, and speciation. In: Bell, M.A., Futuyma, D.J., Eanes, W.F. & Levinton, J.S. (Eds.) *Evolution since Darwin: the first 150 years*. Sunderland, MA: Sinauer Press, pp. 381–420.
Louca, S. & Pennell, M.W. (2020) Extant timetrees are consistent with a myriad of diversification histories. *Nature*, 580, 502–505.
Luiz, O.J., Allen, A.P., Robertson, D.R., Floeter, S.R., Kulbicki, M., Vigliola, L. et al. (2013) Adult and larval traits as determinants of geographic range size among tropical reef fishes. *Proceedings of the National Academy of Sciences*, 110, 16498–16502.
Maddison, W.P. & Fitz John, R.G. (2015) The unsolved challenge to phylogenetic correlation tests for categorical characters. *Systematic Biology*, 64, 127–136.
Matzke, N.J. (2013) *Bio geo BEARS: bio geography with Bayesian (and likelihood) evolutionary analysis in R scripts*. Available at: cran.r-project/web/packages/BioGeoBEARS/ [Accessed January 2020]
Mayr, E. (1960) The emergence of evolutionary novelties. In: Tax, S. (Ed.) *Evolution after Darwin*. Cambridge, MA: Harvard University Press, pp. 349–380.
McCormack, J.E., Faircloth, B.C., Crawford, N.G., Gowaty, P.A., Brumfield, R.T. & Glenn, T.C. (2012) Ultraconserved elements are novel phylogenomic markers that resolve placental mammal phylogeny when combined with species-tree analysis. *Genome Research*, 22, 746–754.
Mezger, D. & Moreau, C.S. (2016) Out of South-East Asia: phylogeny and biogeography of the spiny ant genus *Polyrhachis* Smith (Hymenoptera: Formicidae). *Systematic Entomology*, 41, 369–378.
Miller, M.A., Pfeiffer, W. & Schwartz, T. (2010) Creating the CIPRES science gateway for inference of large phylogenetic trees. In: *Proceedings of the Gateway Computing Environments Workshop (GCE), New Orleans, LA*. New Orleans, Louisiana: Institute of Electrical and Electronics Engineers (IEEE), pp. 1–8.
Mirarab, S., Bayzid, M.S., Boussau, B. & Warnow, T. (2014) Statistical binning enables an accurate coalescent-based estimation of the avian tree. *Science*, 346, 1250463.
Moreau, C.S. (2014) A practical guide to DNA extraction, PCR, and gene-based DNA sequencing in insects. *Halteres*, 5, 32–42.
Moreau, C.S. & Bell, C.D. (2013) Testing the museum versus cradle tropical biological diversity hypothesis: phylogeny, diversification, and ancestral biogeographic range evolution of the ants. *Evolution*, 67, 2240–2257.
Moreau, C.S. & Wray, B.D. (2017) An empirical test of reduced-representation genomics to infer species-level phylogenies for two ant groups. *Insect Systematics and Diversity*, 1, 1–8.
Mundry, R. (2014) Statistical issues and assumptions of phylogenetic generalized least squares. In: *Modern phylogenetic comparative methods and their application in evolutionary biology*. Berlin, Heidelberg: Springer, pp. 131–153.
Nelsen, M.P., Ree, R.H. & Moreau, C.S. (2018) Ant–plant interactions evolved through increasing interdependence. *Proceedings of the National Academy of Sciences*, 115, 12253–12258.
Nguyen, L.T., Schmidt, H.A., Von Haeseler, A. & Minh, B.Q. (2015) IQ-TREE: a fast and effective stochastic algorithm for estimating maximum-likelihood phylogenies. *Molecular Biology and Evolution*, 32, 268–274.

Orme, D., Freckleton, R., Thomas, G., Petzoldt, T., Fritz, S., Isaac, N. et al. (2018) *caper: comparative analyses of phylogenetics and evolution in R*. CRAN: R package v.1.0.1. Available at: https://CRAN.R-project.org/package=caper/

Parr, C.L., Dunn, R.R., Sanders, N.J., Weiser, M.D., Photakis, M., Bishop, T. R. et al. (2017) Global ants: a new database on the geography of ant traits (Hymenoptera: Formicidae). *Insect Conservation and Diversity*, 10, 5–20.

Pekár, S., Petráková, L., Bulbert, M.W., Whiting, M.J. & Herberstein, M.E. (2017) The golden mimicry complex uses a wide spectrum of defence to deter a community of predators. *eLife*, 6, e22089.

Pigot, A.L. & Tobias, J.A. (2013) Species interactions constrain geographic range expansion over evolutionary time. *Ecology Letters*, 16, 330–338.

Price, S.L., Blanchard, B.D., Powell, S., Blaimer, B.B. & Moreau, C.S. (2022) Phylogenomics and fossil data Iiform the systematics and geographic range evolution of a diverse Neotropical ant lineage. *Insect Systematics and Diversity*, 6, 9.

Price, S.L., Powell, S., Kronauer, D.J., Tran, L.A., Pierce, N.E. & Wayne, R.K. (2014) Renewed diversification is associated with new ecological opportunity in the Neotropical turtle ants. *Journal of Evolutionary Biology*, 27, 242–258.

Puttick, M.N. (2019) MCMCtreeR: functions to prepare MCMCtree analyses and visualize posterior ages on trees. *Bioinformatics*, 35, 5321–5322.

QGIS.org. (2020) *QGIS geographic information system*. QGIS Association. Available at: http://www.qgis.org

R Core Team. (2018) *R: a language and environment for statistical computing*. Vienna: R Foundation for Statistical Computing. Available at: http://www.R-project.org/

Rabosky, D.L. (2014) Automatic detection of key innovations, rate shifts, and diversity-dependence of phylogenetic trees. *PLoS One*, 9, e89543.

Rabosky, D.L. & Goldberg, E.E. (2015) Model inadequacy and mistaken inferences of trait-dependent speciation. *Systematic Biology*, 64, 340–355.

Rabosky, D.L., Grundler, M., Anderson, C., Title, P., Shi, J.J., Brown, J.W. et al. (2014) BAMM tools: an R package for the analysis of evolutionary dynamics on phylogenetic trees. *Methods in Ecology and Evolution*, 5, 701–707.

Rabosky, D.L., Mitchell, J.S. & Chang, J. (2017) Is BAMM flawed? Theoretical and practical concerns in the analysis of multi-rate diversification models. *Systematic Biology*, 66, 477–498.

Rambaut, A., Drummond, A.J., Xie, D., Baele, G. & Suchard, M.A. (2018) Posterior summarization in Bayesian phylogenetics using Tracer 1.7. *Systematic Biology*, 67, 901–904.

Ree, R.H. & Sanmartín, I. (2018) Conceptual and statistical problems with the DEC+ J model of founder-event speciation and its comparison with DEC via model selection. *Journal of Biogeography*, 45, 741–749.

Reis, M.D. & Yang, Z. (2011) Approximate likelihood calculation on a phylogeny for Bayesian estimation of divergence times. *Molecular Biology and Evolution*, 28, 2161–2172.

Revell, L.J. (2012) phytools: an R package for phylogenetic comparative biology (and other things). *Methods in Ecology and Evolution*, 3, 217–223.

Revell, L.J. (2013) Two new graphical methods for mapping trait evolution on phylogenies. *Methods in Ecology and Evolution*, 4, 754–759.

Rigato, F. (2016) The ant genus *Polyrhachis* F. Smith in sub-Saharan Africa, with descriptions of ten new species (Hymenoptera: Formicidae). *Zootaxa*, 4088, 1–50.

RStudio Team. (2015) *RStudio: integrated development for R*. Boston, MA: RStudio, Inc. Available at: http://www.rstudio.com/

Rueden, C.T., Schindelin, J., Hiner, M.C., DeZonia, B.E., Walter, A.E., Arena, E.T. et al. (2017) Image J2: image J for the next generation of scientific image data. *BMC Bioinformatics*, 18, 529.

Sarnat, E.M., Friedman, N.R., Fischer, G., Lecroq-Bennet, B. & Economo, E. P. (2017) Rise of the spiny ants: diversification, ecology and function of extreme traits in the hyperdiverse genus *Pheidole* (Hymenoptera: Formicidae). *Biological Journal of the Linnean Society*, 122, 514–538.

Sarnat, E.M. & Moreau, C.S. (2011) Biogeography and morphological evolution in a Pacific island ant radiation. *Molecular Ecology*, 20, 114–130.

Schindelin, J., Arganda-Carreras, I., Frise, E., Kaynig, V., Longair, M., Pietzsch, T. et al. (2012) Fiji: an open-source platform for biological-image analysis. *Nature Methods*, 9, 676–682.

Siemens, D.H., Haugen, R., Matzner, S. & Van Asma, N. (2009) Plant chemical defence allocation constrains evolution of local range. *Molecular Ecology*, 18, 4974–4983.

Stamatakis, A. (2014) RAxML version 8: a tool for phylogenetic analysis and post-analysis of large phylogenies. *Bioinformatics*, 30, 1312–1313.

Suchan, T. & Alvarez, N. (2015) Fifty years after Ehrlich and Raven, is there support for plant-insect coevolution as a major driver of species diversification? *Entomologia Experimentalis et Applicata*, 157, 98–112.

Vamosi, S.M. & Schluter, D. (2004) Character shifts in the defensive armor of sympatric sticklebacks. *Evolution*, 58, 376–385.

Van Dam, M.H., Lam, A.W., Sagata, K., Gewa, B., Laufa, R., Balke, M. et al. (2017) Ultraconserved elements (UCEs) resolve the phylogeny of Australasian smurf-weevils. *PLoS One*, 12, e0188044.

Wallace, A.R. (1863) On the physical geography of the Malay archipelago. *Journal of the Royal Geographical Society of London*, 7, 205–212.

Wappler, T., Dlussky, G.M. & Reuter, M. (2009) The first fossil record of *Polyrhachis* (Hymenoptera: Formicidae: Formicinae) from the Upper Miocene of Crete (Greece). *Paläontologische Zeitschrift*, 83, 431–438.

Weber, M.G. & Agrawal, A.A. (2014) Defense mutualisms enhance plant diversification. *Proceedings of the National Academy of Sciences*, 111, 16442–16447.

Weeks, B.C. & Claramunt, S. (2014) Dispersal has inhibited avian diversification in Australasian archipelagoes. *Proceedings of the Royal Society B*, 281, 20141257.

Wilson, E.O. (1959) Some ecological characteristics of ants in New Guinea rain forests. *Ecology*, 40, 437–447.

Winston, M.E., Kronauer, D.J. & Moreau, C.S. (2017) Early and dynamic colonization of Central America drives speciation in Neotropical army ants. *Molecular Ecology*, 26, 859–870.

Yang, Z. (2007) PAML 4: phylogenetic analysis by maximum likelihood. *Molecular Biology and Evolution*, 24, 1586–1591.

Zhang, C., Rabiee, M., Sayyari, E. & Mirarab, S. (2018) ASTRAL-III: polynomial time species tree reconstruction from partially resolved gene trees. *BMC Bioinformatics*, 19, 153.

Zhang, C., Sayyari, E. & Mirarab, S. (2017) ASTRAL-III: increased scalability and impacts of contracting low support branches. In: *RECOMB international workshop on comparative genomics*. Cham: Springer, pp. 53–75.

Zhang, Y.M., Williams, J.L. & Lucky, A. (2019) Understanding UCEs: a comprehensive primer on using ultraconserved elements for arthropod phylogenomics. *Insect Systematics and Diversity*, 3, 1–12.

SUPPORTING INFORMATION

Additional supporting information can be found online in the Supporting Information section at the end of this article.

Appendix S1: Supporting Information.

Table S1: All taxa (including outgroups) that were sequenced using the UCE pipeline (Faircloth, 2015, 2016), with associated data for each species.

Table S2: Collection details, available voucher information and NCBI accession numbers associated with *Polyrhachis* samples sequenced for this study.

Table S3: Calibration nodes and ages used for divergence dating analyses in MCMCTree.

Table S4: Quality control information for pre-assembly, post-assembly and UCE selection.

Table S5: Information about partition schemes and diagnostics of results under each scheme.

Table S6: Results from *ES-sim* and QuaSSE analyses.

Table S7: Results from phylogenetic generalized least squares (PGLS) analyses including *spine length* and *body size* as predictors of *range size*, and including *body size* and *range size* as predictors of *body size*, for both the MCMCTree and BEAST2-100BEST phylogenies. We conducted two multivariate PGLS analyses for each model—one with zero-spine taxa included, and one with zero-spine taxa excluded.

Figure S1: Examples of spine measurements. Red lines show the path traced using the 'Straight Line' or 'Segmented Line' tools in ImageJ. Species (and photo credit), from top left: (a, b) *P. bellicosa* (Christiana Klingenberg), (c, d) *P. ypsilon* (Zach Lieberman), (e, f) *P. argentosa* (Zach Lieberman), (g, h) *P. emmae* (Will Ericson), (i, j) *P. deceptor* (April Nobile), (k, l) *P. epinotalis* (Bradley Reynolds). From www.antweb.org under a Creative Commons Attribution Licence. Accessed 21 December 2019.

Figure S2: *Polyrhachis* phylogenetic topology inferred with the rclusterf-partitioned dataset in RAxML.

Figure S3: *Polyrhachis* phylogenetic topology inferred using ExaBayes.

Figure S4: ASTRAL-III topology shown alongside the RAxML topology. Differences between the gene-tree and maximum likelihood ingroup topologies are labelled with red boxes.

Figure S5: Time-scaled phylogeny of *Polyrhachis* inferred using MCMCTree with DNA data under the independent rates model.

Figure S6: Time-scaled phylogeny of *Polyrhachis* inferred using MCMCTree without DNA data (i.e., priors-only run) under the independent rates model.

Figure S7: Mean 95% HPD values for with-data and no-data (i.e., priors-only) MCMC runs under the independent rates model, plotted against each other. Note that for each independent run, values clearly deviate from the linear relationship expected if data were not informative.

Figure S8: Time-scaled phylogeny of *Polyrhachis* inferred using MCMCTree with DNA data under the correlated rates model.

Figure S9: Time-scaled phylogeny of *Polyrhachis* inferred using MCMCTree without DNA data (i.e., priors-only run) under the correlated rates model.

Figure S10: Mean 95% HPD values for with-data and no-data (i.e., priors-only) MCMC runs under the correlated rates model, plotted against each other. Note that for each independent run, values do not substantially deviate from the linear relationship expected if data were not informative.

Figure S11: Time-scaled phylogeny of *Polyrhachis* inferred using BEAST2 with the 100-BEST dataset.

Figure S12: Time-scaled phylogeny of *Polyrhachis* inferred using BEAST2 with the 100-RANDOM dataset.

Figure S13: Time-scaled phylogeny of *Polyrhachis* inferred using BEAST2 without DNA data (priors only).

Figure S14: Ancestral state estimation for *relative spine length* implemented using the 'contMap' function in phytools for (a) the MCMCTree phylogeny, and (b) the BEAST2-100BEST phylogeny.

Figure S15: Ancestral state estimation for *relative max spine length* implemented using the 'contMap' function in phytools for (a) the MCMCTree phylogeny, and (b) the BEAST2-100BEST phylogeny.

Figure S16: Ancestral state estimation for *body size* implemented using the 'contMap' function in phytools for (a) the MCMCTree phylogeny, and (b) the BEAST2-100BEST phylogeny.

Figure S17: Ancestral state estimation for *range size* implemented using the 'contMap' function in phytools for (a) the MCMCTree phylogeny, and (b) the BEAST2-100BEST phylogeny.

Figure S18: Results from ancestral range estimation with the MCMCTree phylogeny under the 'BAYAREALIKE' model implemented in BioGeoBEARS.

Figure S19: Results from ancestral range estimation with the BEAST2-100BEST phylogeny under the 'BAYAREALIKE' model implemented in BioGeoBEARS.

Figure S20: Results from a BAMM analysis of the time-scaled BEAST2-100BEST phylogeny. (a) Mean phylorate plot. (b) 95% credible shift set (nine plots representing 0.955 frequency displayed).

Figure S21: Polyrhachis phylogeny inferred in RAxML, with current subgeneric taxonomy displayed. Samples placed in subgenera that differ from current taxonomic designations are highlighted in red.

How to cite this article: Blanchard, B.D. & Moreau, C.S. (2022) Defensive spines are associated with large geographic range but not diversification in spiny ants (Hymenoptera: Formicidae: *Polyrhachis*). *Systematic Entomology*, 1–13. Available from: https://doi.org/10.1111/syen.12578